

Comparative Mechanical Analysis Using Finite Element Model of Material Selection of Hoes

Donghai Huang,¹ Huajie Shen,^{1,2*} Xinzhen Zhuo,¹ Caixia Bai,¹ Kaiqing Shao,² Yifang Jiang,¹ Caiping Lian,¹ Fengwu Zhang,³ Rongfeng Ding,¹ and Yushan Yang⁴

¹School of Design, Fujian University of Technology, Fuzhou 350118, China

²School of Materials and Chemical Engineering, Southwest Forestry University, Kunming 650224, China

³School of Mechanical and Electrical Engineering, Sanming University, Sanming 365004, China

⁴School of Materials and Chemical Engineering, Southwest Forestry University, Kunming 650224, China

(Received March 31, 2025; accepted October 28, 2025)

Keywords: hoeing tools, mechanical properties, ANSYS Workbench, finite element method, comprehensive scoring method

Using the finite element analysis software ANSYS Workbench, we examined the characteristics of materials and selected the best ones for hoes. The mechanical properties of different materials were compared using ANSYS Workbench. Finite element analysis was adopted to evaluate the material combinations for the hoe handle and cutter head and determine the optimal combination for efficient agricultural work. The combinations of ash wood, beech wood, fir wood, cycad wood, and acacia wood, and manganese 13 steel, No.45 steel, and spring steel used for the hoe handle and cutter head were simulated for work efficiency. The work efficiency was then analyzed and compared among the combinations in terms of the stresses on the hoe, the ratio of the simulated stress to the maximum stress, soil impact depth, and soil deformation range. The work efficiency of the hoe was correlated with the horizontal elastic modulus of wood. The computational results of this study are essential for developing an appropriate sensor technology, identifying the optimal placement for strain gauges to experimentally validate the critical high-stress points identified through simulation.

1. Introduction

The hoe is widely used in agriculture. Owing to its simplicity, practicality, and adaptability, it has been a staple tool in agriculture for centuries. Despite the prevalence of mechanization and automation in modern farming, the hoe is still favored by farmers.⁽¹⁾ While metals are increasingly being used, wood remains the primary material for hoe handles. Different ethnic groups in various regions employ various materials for hoe handles based on local availability. For instance, acacia trees are commonly used in northern China, whereas beech trees are preferred in southern regions. Cedar, ash, cycad wood, and sandalwood are also utilized in different areas.^(2,3)

*Corresponding author: e-mail: shenhuajie@fjut.edu.cn
<https://doi.org/10.18494/SAM5680>

Tests comparing new and traditional hoes reveal differences in their impact on middle-aged female farmers' heart rates and work performance. The new hoe significantly improved the farmers' efficiency, with the majority expressing a preference for the shorter hoe over the longer one.⁽⁴⁾ In this study, computational analysis was conducted using the finite element method (FEM).^(5,6)

FEM is mainly used for evaluating the mechanical properties of devices and analyzing the working conditions and engineering characteristics of tools. For example, Dai studied the structure and mechanisms of sofa frames using FEM,⁽⁷⁾ Kasal simulated the strengths of various sofa frames,⁽⁸⁾ and Smardzewski *et al.* assessed the stiffness of upholstered furniture joints using FEM.⁽⁹⁾ SolidWorks is used to investigate the mechanical properties of deformed furniture structures based on FEM.⁽¹⁰⁾ The finite element mechanical analysis is inherently dependent on sensor-derived data for its inputs and validation. NIR sensors are widely used to characterize the material parameters of wood, providing accurate horizontal elastic modulus (ET) values.⁽¹¹⁾ For dynamic testing, inertial measurement units are used for measuring the tool's velocity and acceleration during the hoeing stroke, and quantifying the kinetic energy and impact forces used as boundary conditions in the simulation.⁽¹²⁾ These sensors need to be placed at the high-stress areas identified by FEM results (such as the junction between the handle and the cutter head) to measure the real-time localized stress and force experienced during agricultural work, ensuring structural integrity predictions.

We analyzed the work efficiency of hoe handles and cutter heads with different materials. By FEM, we identified the advantages and disadvantages of different materials used for hoes. The degree of soil deformation was simulated for hoes with various materials. Additionally, the stress on hoes was simulated to estimate the work efficiency. By FEM, we identified the advantages and disadvantages of different materials used for hoes. The stress on hoes was simulated to estimate the work efficiency. The findings of this study offer a reference for selecting appropriate materials for hoes and identifying the structural areas and expected stresses, thereby establishing the theoretical basis for developing an appropriate sensor technology (such as strain gauges) required for subsequent experimental validation and real-time field data acquisition.

2. Materials and Methods

2.1 Material selection and performance parameters

A hoe comprises a cutter head, spigot, and handle (Fig. 1). One end of the hoe handle is typically cylindrical, while the other end is designed to fit into a hole, where it is secured to the cutter head using mortise and tenon joints. One end of the cutter head is used to cut, while the other end is connected to the mortise and tenon joints, and the hoe handle. Wedge-shaped pins are inserted to flexibly connect the hoe handle and cutter head. Sometimes, the hoe handle and cutter head are welded. Common materials for the hoe's cutter heads are manganese 13 (Mn13) steel and No.45 steel (carbon structural steel), while those for the hoe's handles include spring steel, ash wood, beech wood, fir wood, cycad wood, and acacia wood.

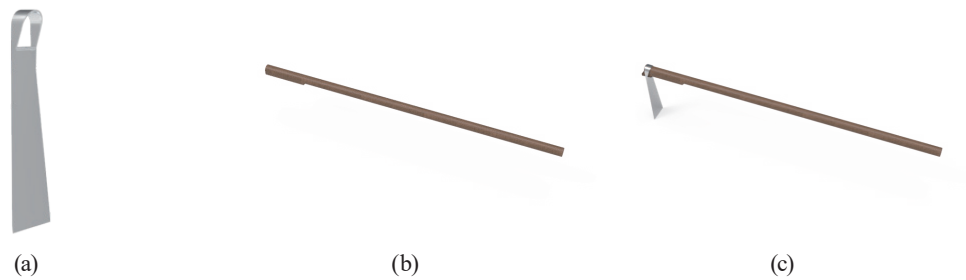


Fig. 1. (Color online) Typical hoe used in agriculture. (a) Cutter head, (b) hoe handle, and (c) complete hoe.

The physical and mechanical properties of the materials used to make hoes are summarized in Tables 1 and 2.^(13–18) Wood is an anisotropic material, and wood cells and tissues grow parallel to the axial axis of the trunk. The main cellular assemblies form into concentric rings in the trunk, which gives wood its orthogonal symmetry.⁽¹⁷⁾ The properties of orthotropic anisotropic materials, such as wood, are determined using the following parameters: three moduli of shear elasticity, three Poisson's ratios, and moisture content. These are usually measured by NIR sensors. The physico-mechanical parameters of the soil in this study were a soil density of 1.330 g/cm³, an ET of 4.54 MPa, and Poisson's ratio of 0.410.⁽¹⁹⁾

2.2 FEM

A 3D model of the hoe was created using SolidWorks. The boundary conditions of the hoe under working conditions were defined through experiments. A camera was used to record the cycle of the work using hoe, and the velocity when the hoe touched the ground was measured from the video. The model was imported into ANSYS Workbench. The combination of materials experimented with in this study included ash wood + Mn13 steel, ash wood + No.45 steel, ash wood + spring steel, beechwood + Mn13 steel, beechwood + No.45 steel, beechwood + No.45 steel, beechwood + spring steel, fir wood + Mn 13, fir wood + No.45 steel, fir wood + No.45 steel, fir wood + spring steel steel, fir wood + No.45 steel, fir + spring steel, cycad wood+ manganese 13, cycad wood + No.45 steel, cycad wood + spring steel, acacia wood + Mn13 steel, acacia wood + No.45 steel, and acacia wood + spring steel.

2.3 Mechanical analysis

A farmer grips a hoe with both hands. Owing to the limited and variable swing of the backhand (far blade end) among individuals, the backhand contact point is treated as a fixed point within the boundary conditions. The contact point of the front hand (near the end of the cutter head) is regarded as the force application point, and the force F_1 perpendicular to the hoe handle moves the hoe downward. The force at the contact point of the backhand is decomposed into F_x and F_y in the horizontal and vertical directions, respectively, and supports the hoe to rotate around the point counterclockwise on the soil. Upon contact with the soil, F_2 is exerted on the cutter head F_2 . The force analysis result is shown in Fig. 2.

Table 1

Physical and mechanical parameters of materials used for hoe handles.

Material	Ash wood	Beech wood	Fir wood	Cycad wood	Acacia wood
Species	Oleaceae <i>Fraxinus chinensis</i> Roxb	Ulmaceae <i>Zelkova schneideriana</i> Hand-Mazz	Taxodiaceae <i>Cunninghamia lanceolata</i> Lamb Hook	Fagaceae <i>Cyclobalanopsis glauca</i> Thunb. Oerst.	Leguminosae <i>Sophora japonica</i> L.
Density (g/cm ³)	0.67	0.75	0.39	0.705	0.78
Modulus of elasticity of grain eyre (MPa)	15790	13700	11583	16285	12753
Horizontal radial modulus of elasticity (MPa)	1516	2240	896	1715	1342
Horizontal tangential modulus of elasticity (MPa)	827	1140	496	880	690
Grain diameter surface shear modulus of elasticity (MPa)	896	1060	690	953	852
Shear ET of linear chord surface (MPa)	1310	1610	758	1482	1354
Horizontal shear modulus of elasticity (MPa)	269	460	39	331	315
Ten-direction pressure strain/ <i>R</i> -direction extension strain (μRT)	0.71	0.75	0.43	0.72	0.73
Pressure strain in <i>R</i> -direction / Extended strain in <i>L</i> -direction μLR	0.46	0.45	0.37	0.44	0.47
Compressive strain in <i>R</i> -direction/ Extended strain in <i>L</i> -direction μLT	0.51	0.51	0.47	0.52	0.51
Flexural strength (MPa)	112	128	75	142	124
Compressive strength (MPa)	49	48	38	65	53

Table 2

Physical and mechanical parameters of materials for cutter heads.

Material	Density (g/cm ³)	ET (MPa)	Poisson's ratio	Ultimate strength (MPa)	Yield strength (MPa)
Mn13 steel	7.791	2.1×10^5	0.3	736	440
No.45 steel	7.850	2.09×10^5	0.269	600	355
Spring steel	7.810	2.06×10^5	0.285	1765	1570

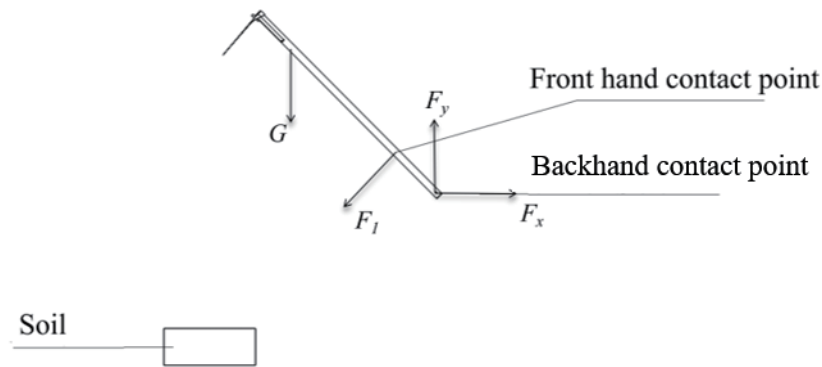


Fig. 2. Analysis of force when using hoe.

To verify the components of the hoe in a safe state when the hoe is subjected to force, the structural strength and permissible stress of the materials were analyzed. The structural strength of the material is the capability of the material to resist the stresses applied to it without damage.⁽²⁰⁾ The materials used were wood and steel. The strength of the wood is determined under specific conditions, considering the variability, defects, long-term loading, and overloading of wood, which are the factors that affect the material strength. The stress applied to wood is calculated as

$$[\sigma] = \sigma_{min} \cdot K_1 \cdot K_2 \cdot K_3 \cdot K_4 \cdot \frac{1}{K_5 \cdot K_6}. \quad (1)$$

Here, σ denotes the allowable stress of wood in MPa, σ_{min} denotes the lowest strength of wood in MPa, K_1 denotes the stress due to the long-term action of the load, K_2 denotes the stress defect of the wood, K_3 denotes the stress by the dryness of the wood, K_4 denotes the stress on the wood, K_5 denotes the standard load, and K_6 is the factor that increases the internal force. The coefficients of the factors for the strength of different types of wood are shown in Table 3.⁽¹⁷⁾

The stress of steel is calculated

$$[\sigma] = \frac{\sigma_s}{n}, \quad (2)$$

where σ is the allowable stress of the material, σ_s is the yield limit of the material, and n is the safety factor of the material. The safety factor of steel in this study was 1.8.

The stresses of various materials calculated using Eqs. (1) and (2) were as follows: 37.12 MPa for ash wood, 36.36 MPa for beechwood, 28.79 MPa for cedar wood, 49.24 MPa for cycad wood, and 40.15 MPa for acacia wood. The stresses of Mn13, No.45 steel, and spring steel were 244.44, 197.22, and 872.22 MPa, respectively.

Table 3
Effects of coefficients of factors on wood strength.

Parameters	K_1	K_2	K_3	K_4	K_5	K_6
Anti-compressiveness	—	—	1.00	—	1.20	1.10

3. Results

3.1 Finite element meshing

The number of meshes affects the accuracy and calculation time of FEM. In the experiment, the mesh should be defined to ensure accurate results and quick calculations.⁽²¹⁾ In the model, the hoe was assumed to have a tetrahedral unit with a size of 10 mm. The unit mesh size was 1 mm for the blade of the cutter head and was adjusted to 5 mm for the refinement of the mesh. The soil was also meshed in hexahedral solid units with a size of 20 mm.^(22,23) Considering the friction between the elements of the hoe, an augmented Lagrangian algorithm was constructed to increase the contact area of the surfaces and the insertion of the cutter head into the hoe handle.⁽²⁴⁾ After meshing, the hoe model contained 7196 nodes and 27095 cells, whereas the soil model had 54621 nodes and 50000 cells.

3.2 Stress analysis

Stress is the set of distributed internal forces at a point on the cross section. By estimating the stress and comparing it with the maximum stress, Ebrahimi determined if the strength of the structure met the required condition.⁽²⁵⁾ A tiny circular hole was drilled at the backhand contact point to connect a rotary-connecting vice to the cutter head. At the forehand contact point, FI was set to 15 N as a constant force, while the actual force might vary. The velocity when the hoe touched the ground was assumed to be the same as that in the real situation. Since gravitational force acts on the hoe, different masses of hoes result in different forces depending on the materials used. To eliminate the effect of different masses, an equal force (10 N) was assumed to be applied to the cutter head and the surface of the soil.

The Lagrangian Solver Dynamic (LS-DYNA) module in ANSYS Workbench simulated the entire process of using the hoe and subsequent rebound and the stress change of the blade of the cutter head from their initial drop to soil contact.⁽²⁶⁾ Figure 3 shows the change in cutter head stress from the maximum to the minimum. The hoes with different materials showed different stress peaks at different points in the impact process on the soil. Assuming the force applied to the hoe was equal, hoes with different materials had different densities. Therefore, the lighter the hoe, the greater the acceleration, and the shorter the time to soil impact.

Figure 3 shows the results of the von Mises stress distribution across 15 different materials and a strap, hook, or connector of the hoes. The von Mises stress is used to predict the yielding or failure of ductile materials under multiaxial loading. The color contour plots illustrate where the stresses are concentrated and their values.

The maximum stress (red/yellow color range) is concentrated around the loop/opening at the top. This indicates that this area, where the component is attached or loaded, is the critical

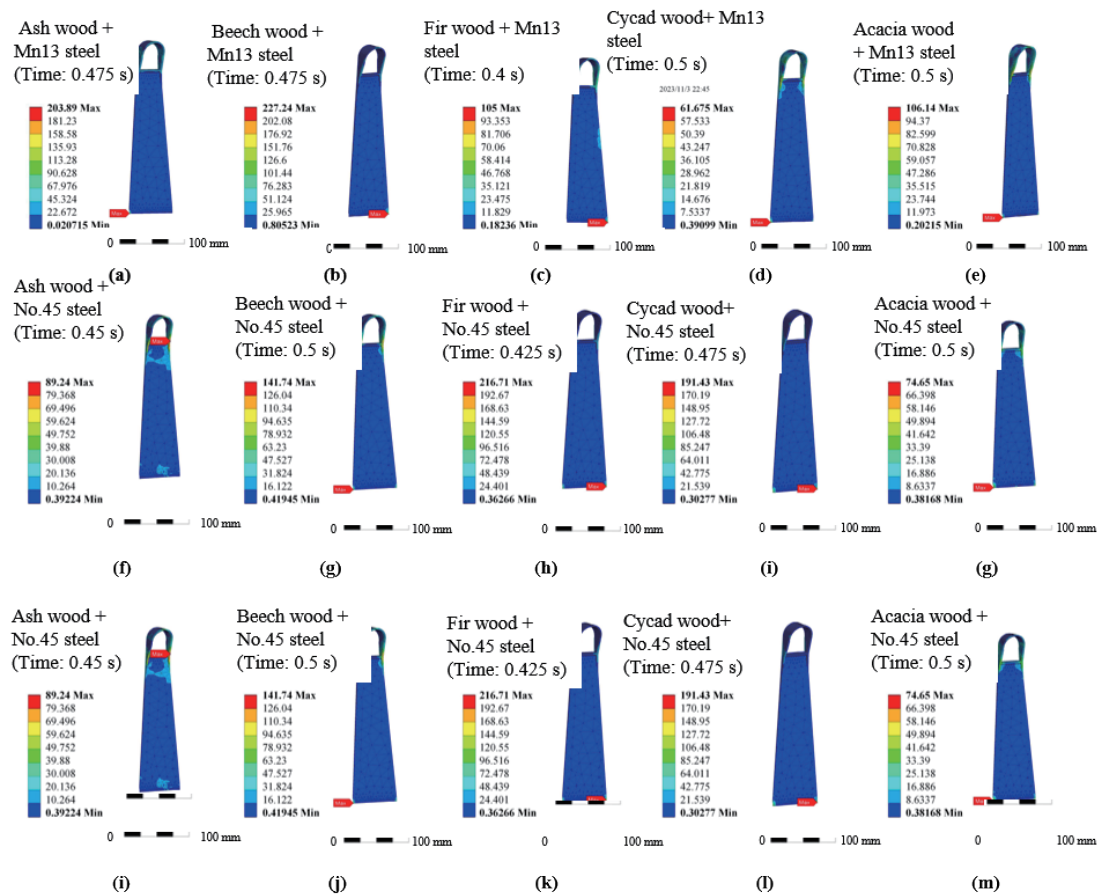


Fig. 3. (Color online) Maximum stresses of cutter head of hoes and hoe handle with different combinations of wood and steel. Red marks indicate the parts subject to maximum stress.

failure point in all designs. The highest stresses were observed in Ash + Mn13 steel and Beech + Mn13 steel, with maximum stresses of 203.89 and 227.24 MPa, respectively. This suggests that the beech with Mn13 steel is the most stressed configuration and, therefore, the most likely to fail if the applied load is high. The lowest maximum stress was found in Beech + Spring steel at 51.808 MPa. This design is the most structurally efficient in handling the applied load without high stress concentrations, making it the most robust option among the tested configurations.

Mn13 steel generally resulted in the highest stresses (the maximum stress of 227.24 MPa), and No.45 steel showed intermediate stress levels (the maximum of 206.76 MPa). Spring steel showed the lowest stresses (the maximum of 160.01 MPa, and most were less than 115 MPa). This suggests that the lower stiffness or different yield properties of spring steel may distribute the load more favorably (Table 4).

3.3 Soil deformation

The depth of the hoe's penetration into the soil was used as an indicator of soil deformation in this study. Under the same boundary condition, hoes with different materials showed different

Table 4
Maximum stresses of different materials.

Material	Symbol	Maximum stress (MPa)
Ash wood + Mn13 steel	A1	203.89
Ash wood + No.45 steel	A2	89.24
Ash wood + Spring steel	A3	95.135
Beech wood + Mn13 steel	B1	227.24
Beech wood + No.45 steel	B2	141.74
Beech wood + Spring steel	B3	51.808
Fir wood + Mn13 steel	C1	105
Fir wood + No.45 steel	C2	206.76
Fir wood + Spring steel	C3	78.256
Cycad wood + Mn13 steel	D1	61.678
Cycad wood + No.45 steel	D2	191.49
Cycad wood + Spring steel	D3	113.51
Acacia wood + Mn13 steel	E1	106.14
Acacia wood + No.45 steel	E2	74.65
Acacia wood + Spring steel	E3	160.01

penetration depths. Even though the external force moving the hoe was equal, hoes with different materials had different energy levels transferred.⁽²⁷⁾ The greater the soil deformation, the greater the loss of energy in the energy transfer process, indicating that the work efficiency of the hoe was higher. Figure 4 shows the maximum soil deformation range in the process of hoes impacting the soil. The soil deformation range was from 18 to 32 mm, and the hoe with ash wood, beechwood, and cycad wood showed wider ranges, while those with cedar and acacia wood showed narrower ranges. The range of soil deformation by the hoe with ash wood + No.45 steel was 31.93 mm, and that with acacia wood + spring steel was 18.31 mm. The maximum range of the hoes with material combinations was around 30 mm.

We conducted the regression analyses of density, elasticity, shear elasticity, and Poisson's ratios, and the results are shown in Table 5. The linear regression equation used is presented as

$$X = 21.417 + 0.0087 \cdot E_T. \quad (3)$$

Here, X is the deformation of the soil upon the impact of the hoe and E_T is the horizontal ET of the wood structure.

These parameters were positively correlated with the horizontal ET of the wood structure of the materials used in the hoe handles. The larger the ET of the wood structure in the hoeing tools, the larger the impact on the soil. The correlation between the depth of hoeing and the properties of the material was not significant. However, the properties of the anisotropy of the wood used for the hoe handle affected the work efficiency of the hoe significantly.

4. Discussion

The stress and the maximum deformation of the soil by the hoe with different materials were simulated using FEM and ANSYS Workbench. Hoes with different combinations of materials showed different stresses and deformations of the soil.

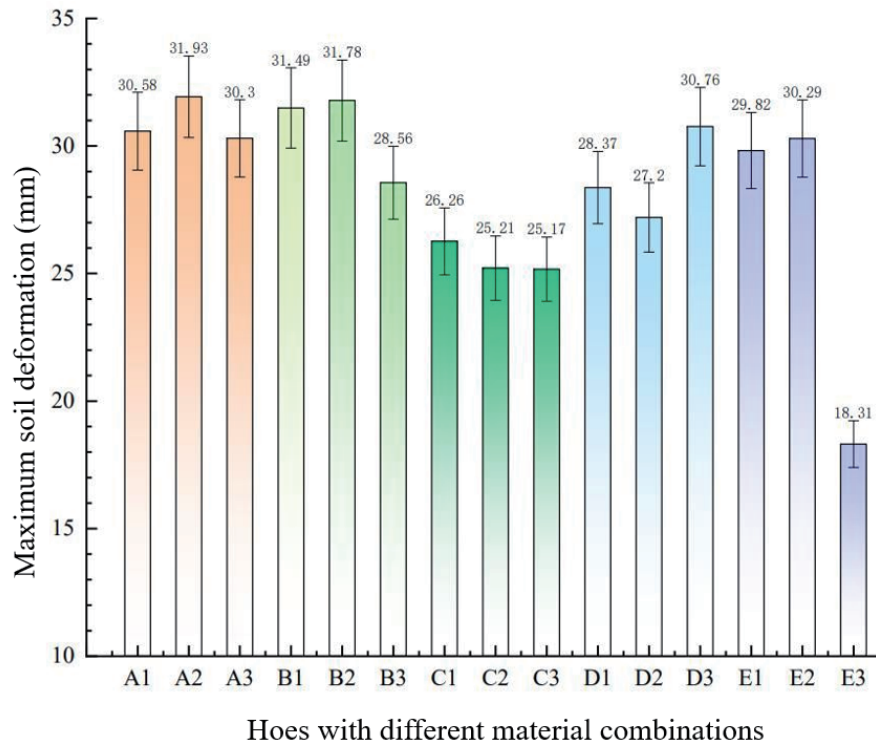


Fig. 4. (Color online) Maximum soil deformation by hoes with different material combinations.

The smaller the ratio of the simulated stress to the maximum stress, the easier the hoe is broken. By comparing the ratio, the strength of the hoe is evaluated. The maximum stresses of hoes with different combinations of wood and steel showed varied stresses and degrees of deformation on the soil. With a good hoe, a farmer can dig deeper with the same external force. In other words, the farmer can save energy for the same amount of work. Therefore, the performance with a hoe should be evaluated. In this study, three indicators of soil deformation were scored: depth and the ratios of the simulated stress to the maximum stresses of wood and steel.⁽²⁸⁾ Twelve tests were conducted and scored as follows.

$$W = \frac{X - X_{min}}{X_{max} - X_{min}} + \left(1 - \frac{Y - Y_{min}}{Y_{max} - Y_{min}}\right) + \left(1 - \frac{Z - Z_{min}}{Z_{max} - Z_{min}}\right) \quad (4)$$

Here, W is the score, X is the soil deformation value at each test, X_{max} is the maximum value of soil deformation, X_{min} is the minimum value of soil deformation, Y is the ratio of the stress to the maximum stress of steel, Y_{max} is the maximum stress of steel, Y_{min} is the minimum stress of steel, Z is the ratio of the simulated stress to the maximum stress of wood, Z_{max} is the maximum stress of wood, and Z_{min} is the minimum stress of wood. The results are presented in Table 6.

The scores of hoes with different materials are shown in Fig. 5. The material combinations of ash wood, cycad wood, and acacia wood scored higher than those of other types of wood. The material combination of spring steel scored higher than those of Mn13 and No.45 steel. For the hoe handle and cutter head, cycad wood + spring steel was the optimal combination.

Table 5

Regression analysis results of parameters for soil deformation upon impact.

Parameter	<i>B</i>	Standard error	<i>t</i>	<i>R</i> ²	<i>F</i>	<i>P</i>	Distinctiveness
Wood density (g/cm ³)	7.5926	6.5777	1.1543	0.0930	1.3324	0.2692	Not significant
Modulus of elasticity (MPa)	9.0842×10^{-4}	4.7844×10^{-4}	1.8987	0.2171	3.6052	0.0800	Not significant
Horizontal radial modulus of elasticity (MPa)	0.0039	0.0019	2.0798	0.2497	4.3258	0.0579	Not significant
Horizontal tangential modulus of elasticity ET (MPa)	0.0087	0.0038	2.2570	0.2815	5.0939	0.0419	Significant
Grain radial surface shear modulus of elasticity (MPa)	0.0144	0.0068	2.1106	0.2552	4.4547	0.0547	Not significant
Shear modulus of elasticity of linear chord (MPa)	0.0052	0.0030	1.7377	0.1885	3.0194	0.1059	Not significant
Horizontal shear modulus of elasticity (MPa)	0.0106	0.0064	1.6570	0.1744	2.7455	0.1215	Not significant
Ten-direction pressure strain/ <i>R</i> -direction extension strain μ RT	11.8069	7.3602	1.6042	0.1652	2.5733	0.1327	Not significant
Pressure strain in <i>R</i> -direction/Extended strain in <i>L</i> -direction μ LR	32.6093	25.6695	1.2704	0.1104	1.6138	0.2262	Not significant
Compressive strain in <i>T</i> -direction/Extended strain in <i>L</i> -direction μ LT	77.6053	50.9614	1.5228	0.1514	2.3190	0.1518	Not significant
Steel density (g/cm ³)	9.9570	39.1277	0.2545	0.0050	0.0648	0.8031	Not significant
Modulus of elasticity of steel <i>E</i> (MPa)	7.2092×10^{-4}	5.3110×10^{-4}	1.3574	0.1241	0.0568	0.1977	Not significant
Poisson's ratio of steel	-1.1442	76.2003	-0.0150	0.0001	0.0002	0.9882	Not significant

(*B* is the regression coefficient at *P* = 0.05. *R*² is the correlation coefficient representing the explanatory strength of the independent variable to the dependent variable.)

The role of sensor technology is critical to the accurate mechanical analysis of agricultural tools. While this comparative FEM study set the loading forces for standardization (*F*₁ = 15 and 10 N impact force), the initial condition for simulation and the velocity of the hoe upon soil contact were monitored by video analysis. Furthermore, density and elastic moduli are conventionally measured using sensors, such as those using NIR sensors. This mechanical analysis identifies the beech wood + spring steel combination (B3) as the most structurally efficient (lowest maximum stress) and cycad wood + spring steel (D3) as the optimal combination for overall work efficiency. These results provide the theoretical basis for developing and positioning appropriate sensor technologies for future research. Specifically, strain gauges or pressure sensors can be placed at the critical high-stress area (top loop opening) to experimentally validate the simulation results and measure actual forces/strains during real-world fieldwork, which is a necessary next step for this research domain.

Table 6
Scores of work efficiency of hoes with different materials.

Material combination	Maximum stress of steel structure (MPa)	Maximum stress of timber structure (MPa)	Maximum soil deformation (mm)	Simulated/maximum stress of steel	Simulated/maximum stress of wood	Overall score
A1	203.89	41.05	30.58	0.83411	1.10587	1.16
A2	89.24	22.82	31.93	0.45249	0.61476	2.38
A3	95.14	23.19	30.30	0.10908	0.62473	2.57
B1	227.24	30.33	31.49	0.92964	0.83416	1.55
B2	141.74	27.44	31.78	0.71869	0.75468	1.90
B3	51.81	30.66	28.56	0.05940	0.84323	2.16
C1	105.00	23.86	26.26	0.42955	0.82876	1.65
C2	216.71	23.47	25.21	1.09882	0.81521	0.95
C3	78.27	15.99	25.17	0.08974	0.55540	2.32
D1	64.68	24.48	28.37	0.26460	0.45654	2.54
D2	191.43	29.40	27.20	0.97064	0.59870	1.56
D3	113.54	27.46	30.76	0.13017	0.55768	2.69
E1	106.14	23.20	29.82	0.43422	0.57783	2.30
E2	74.65	27.64	30.29	0.37851	0.68842	2.22
E3	160.01	21.46	18.31	0.18345	0.53450	1.76

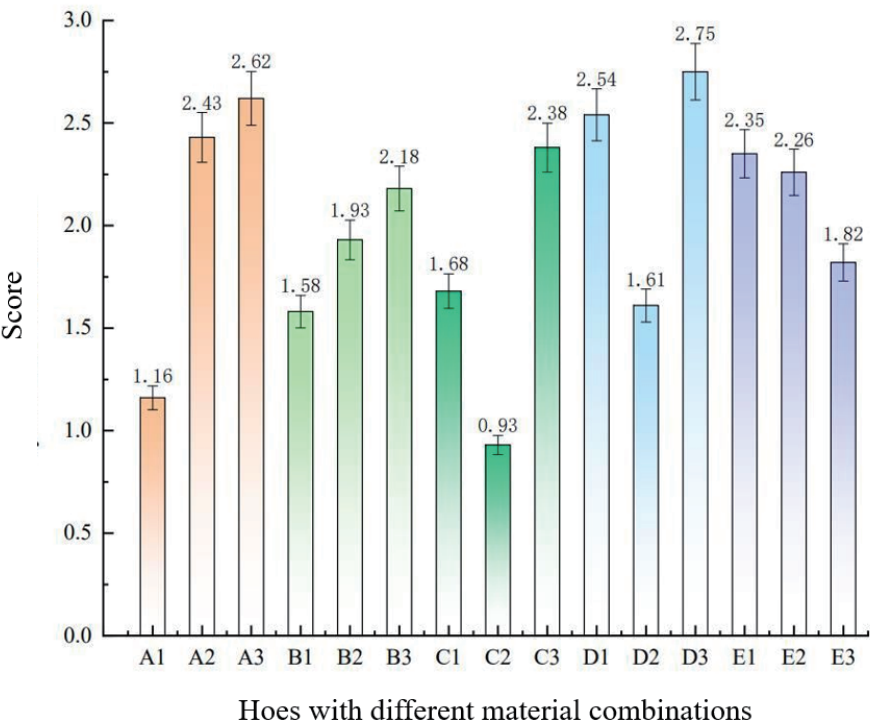


Fig. 5. (Color online) Scores of work efficiency of hoes with different materials.

5. Conclusion

We analyzed the work efficiency of hoes with different materials using FEM. For the hoe handle, ash wood, cycad wood, and acacia wood were more appropriate than fir wood and beech wood, while spring steel was better for the cutter head than Mn13 and No.45 steel. The combination of a cycad wood handle and a spring steel cutter head showed the highest work efficiency. The work efficiency of the hoe was closely related to the ET of the wood structure.

We only considered the wood with a particular moisture content in this study, which necessitates further study on the work efficiency of the hoe with wood with different moisture contents. The production costs of the hoe should also be considered. As only five types of wood and three types of steel were experimented with in this study, more diverse materials need to be studied. At the same time, other structural elements of the hoe must be included in the simulation to enrich the research results.

The findings of this computational study underscore the relationship between mechanical analysis and sensor technology in agricultural tool design. Specifically, FEM was used to identify the critical high-stress area (the connection point of the cutter head and handle). The results are applicable to the following research, where sensor technology is critical. The precise stress patterns and maximum values determined enable the exact specifications required for developing, calibrating, and strategically placing appropriate force or strain sensors to accurately measure real-world loading during agricultural work. Therefore, the results of this study provide a theoretical basis for developing and choosing appropriate materials and sensor technology for agricultural tools and instruments.

Acknowledgments

This research was funded by the Major Project of Fujian Provincial Social Science Research Base (Project Approval Number: FJ2023JDZ056) and the Fujian Provincial Natural Science Foundation Project (Project Approval Number: 2024J01834).

References

- 1 K. Chandrasekaran, D. Veeraragavathatham, D. Karpagam, and S. A. Firdouse: *Indian J. Tradit. Knowl.* **8** (2009) 212. https://www.researchgate.net/publication/296756523_Traditional_tools_in_agricultural_practices
- 2 Q. Wang: *Bt. Res.* **9** (2020) 409. <https://doi.org/10.12677/br.2020.94052>
- 3 C. Cao and J. Tao: *Sustainability* **13** (2021) 1493. <https://doi.org/10.3390/su13031493>
- 4 L. Vanderwal, R. Rautiainen, R. Kuye, C. Peek-Asa, T. Cook, M. Ramirez, K. Culp, and K. Donham: *Appl. Ergon.* **42** (2011) 749. <https://doi.org/10.1016/j.apergo.2010.12.002>
- 5 W. Hu, W. Fu, and Y. Zhao: *Wood. Res.* **69** (2024) 50. <http://dx.doi.org/10.37763/wr.1336-4561/69.1.5059>
- 6 M. Pucci, R. Spina, and S. Zanforlin: *Energies* **17** (2024) 2366. <https://doi.org/10.3390/en17102366>
- 7 L. Dai: *Theses and Dissertations* (2007). <https://scholarsjunction.msstate.edu/cgi/viewcontent.cgi?article=2299&context=td>
- 8 A. Kasal: *G. U. J. Sci.* **19** (2010) 191. <https://dergipark.org.tr/tr/download/article-file/83088>
- 9 J. Smardzewski, R. Klos, and B. Fabisiak: *Turk. J. Agric. For.* **6** (2013) 802. <http://dx.doi.org/10.3906/tar-1206-8>
- 10 Solidworks: <https://www.solidworks.com/solution/solidworks-makers/cad-furniture-design> (accessed March 2025).
- 11 M. Mancini, W. Leoni, M. Noceetti, C. Urbinati, D. Duca, M. Brunetti, and G. Toscano: *J. Agric. Eng.* **50** (2019) 191. <https://doi.org/10.4081/jae.2019.953>

- 12 N. G. Punchihewa, S. Miyazaki, E. Chosa, and G. Yamako: *Sensors* **20** (2020) 7331. <https://doi.org/10.3390/s20247331>
- 13 China National Standards: https://gbstandards.org/GB_Search.asp?word=spring (accessed March 2025).
- 14 A. S. Bai, A. Y. Jiao, and S. M. Liu: *AMM* **215–216** (2012) 717. <http://dx.doi.org/10.4028/www.scientific.net/AMM.215-216.717>
- 15 Y. Li, C. Yu, W. Zhao, Z. Gao, and L. Du: *Chin. J. Mater. Res.* **39** (2025) 21. <https://www.cjmr.org/EN/10.11901/1005.3093.2024.146>
- 16 FAO: <https://www.fao.org/4/xii/0955-b4.htm> (accessed March 2025).
- 17 H. Li, Z. Zhang, C. Li, Q. Gui, Z. Liu, H. Li, and Z. Jia: *Quat. Sci.* **42** (2022) 172. <https://doi.org/10.11928/j.issn.1001-7410.2022.01.14>
- 18 W. Hu and B. Chen: *Forests* **12** (2021) 478. <http://dx.doi.org/10.3390/f12040478>
- 19 F. Wnag, N. Chang, Z. Zhang, and B. Wang: *Trans. Chin. Soc. Agric. Mach.* **55** (2024) 10. <http://dx.doi.org/10.6041/j.issn.1000-1298.2024.S2.002>
- 20 Z. Duan, Q. Zu, and F. Rao: *Sustainability* **16** (2024) 5357. <https://doi.org/10.3390/su16135357>.
- 21 Y. Zhang: *AMNS* **9** (2024) 1. <http://dx.doi.org/10.2478/amns-2024-1670>
- 22 P. Putrayudanto, J. Lai, P.-P. Song, Y.-C. Tsai, and C.-H. Hsu: *Eng. Computation* **40** (2024) 3765. <https://doi.org/10.1007/s00366-024-01999-9>
- 23 S. Zhang, G. Xu, H. Wu, R. Gu, L. Qi, and Y. Pang: *Eng. Computation* **40** (2024) 1. <http://dx.doi.org/10.1007/s00366-023-01925-5>
- 24 L. Elek, Z. Kovács, L. Csóka, and C. Argarwal: *Eur. J. Wood Prod.* **78** (2020) 351. <https://link.springer.com/article/10.1007/s00107-020-01509-w>
- 25 F. Ebrahimi: *Mechanics of Auxetic Materials and Structures*, F. Ebrahimi, Ed. (Taylor & Francis Group, Abingdon, 2024) Chap. 1.
- 26 D. Liu, C. Dai, Y. Chenggang, and Y. Ma: *Water* **14** (2022) 2808. <https://www.mdpi.com/2073-4441/14/18/2808#>
- 27 J. M. Gorji, G. Payganeh, and R. Moradi-Dastjerdi: *Mech. Based Des. Struct. Mach.* **52** (2024) 2316. <http://dx.doi.org/10.1080/15397734.2023.2177863>
- 28 J. Song, Z. Song, and R. Sun: *Procedia Eng.* **31** (2012) 739. <https://doi.org/10.1016/j.proeng.2012.01.1095>

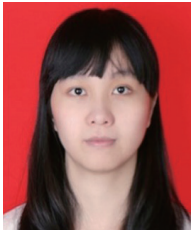
About the Authors



Donghai Huang received his B.S. degree from East China Normal University in 1995 and his M.S. degree from Central South University in 2008. From 2005 to 2009. Since 1995, he has been a teacher at Fujian University of Technology and has served as an assistant, lecturer, and associate professor. His research interests are in environmental design and sensors. (huangdonghai@fjut.edu.cn)



Huajie Shen received his M.S. degree in design from Central South University of Forestry and Technology in 2011 and his Ph.D. degree in wood science and technology from Southwest University of Forestry in 2020. From 2011 to 2021, he was a teacher at Southwest Forestry University and served as an assistant, lecturer, and associate professor. Since 2022, he has been an associate professor at Fujian University of Technology in China. His research interests include the design and manufacturing of wood products and artificial intelligence. (shenhuajie@fjut.edu.cn)



Xinzhen Zhuo received her B.S. degree in visual communication design from Fuzhou University in 2008 and her M.S. degree from Hunan University in 2011. Since 2011, she has been a teacher at Fujian University of Technology and has served as an assistant and lecturer. Her research interests are in visual communication design and sensors. (zhuoxinzhen@fjut.edu.cn)



Caixia Bai received her B.S. degree in management from Kunming Medical University in 2020, served as a medical representative specialist of Abbott from 2020 to 2024, and has been studying for a master's degree in design at Fujian University of Technology since 2024, with research interests in product design and artificial intelligence. (2242007004@smail.fjut.edu.cn)



Kaiqing Shao received his B.A. degree in horticulture from Yichun University. Since 2022, he has been a postgraduate student majoring in mechanical engineering at Southwest Forestry University. His main research interests are in digital design and manufacturing, and industrial design. (2821824890@qq.com)



Yifan Jiang received her B.A. degree in environmental art design from Xihua University, China, in 2009 and her master's degree in architectural design from Aichi Institute of Technology, Japan, in 2013. Since 2021, she has been a lecturer at Fujian University of Technology in China. Her research interests include cultural and creative product design, interior design of architecture, and environmental art design. (63202101@fjut.edu.cn)



Caiping Lian received her B.Sc. and M.Sc. degrees in wood science and technology from Nanjing Forestry University in 2007 and 2014, respectively. She later obtained her Ph.D. degree in wood science and technology from the Chinese Academy of Forestry in 2020, specializing in bamboo material properties. From 2020 to 2023, she conducted postdoctoral research at the School of Furniture and Industrial Design, Nanjing Forestry University. Since 2023, she has been a lecturer at the School of Design, Fujian University of Technology. Her research interests include bamboo material properties, Kansei engineering of bamboo products, and bamboo product design and development. (liancaiping@fjut.edu.cn)



Fengwu Zhang received his B.S. and M.S. degrees in mechanical engineering from Taiyuan Institute of Technology in 2020 and Southwest Forestry University in 2023, respectively. Since 2023, he has been a teaching assistant at Sanming University, with research interests in industrial design and education, and teaching evaluation. (20230368@fjsmu.edu.cn)



Ding Rongfeng received his B.S. degree from Central South University of Forestry and Technology in 2002. Since 2002, he has been a teacher at Fujian University of Technology and has served as an assistant and lecturer. His research interests are in environmental design and sensors. (dingrongfeng@fjut.edu.cn)



Yang Yushan received his Ph.D. degree in forestry engineering from Zhejiang A & F University in 2023. He joined Southwest Forestry University in 2023. His research focuses on wood science, including wood structure and wood properties, wood moisture and drying, wood protection and improvement, wood recombination and compounding, wood dissociation and assembly, and wood deconstruction and transformation. (yangyushan@swfu.edu.cn)